

# Using hemodynamic parameters quantified with computational fluid dynamics to explore potential mechanisms of occurrence and progression in Alzheimer Disease

**Jian Xie**

Department of Neurology, Affiliated Zhongda Hospital, School of Medicine, Southeast University

**Zaiheng Cheng**

Shenzhen Institutes of Advanced Technology, Chinese Academy of Science

**LiHua Gu**

Department of Neurology, Affiliated ZhongDa Hospital, School of Medicine, Southeast University

**Bokai Wu**

Shenzhen Institutes of Advanced Technology Chinese Academy of Sciences

**Gao-jia Zhang**

Department of Neurology, Nanjing Lishui people's Hospital

**Wen-Shin Shiu**

Shenzhen Institutes of Advanced Technology Chinese Academy of Sciences

**Rongliang Chen**

Shenzhen Institutes of Advanced Technology Chinese Academy of Sciences

**Zan Wang**

Department of Neurology, Affiliated ZhongDa Hospital, School of Medicine, Southeast University

**Chang Liu**

Shenzhen Institutes of Advanced Technology Chinese Academy of Sciences

**Xiao-chuan Cai**

Shenzhen Institutes of Advanced Technology Chinese Academy of Sciences

**Li-Ping Wang**

Shenzhen Institutes of Advanced Technology Chinese Academy of Sciences

**Jia Liu** (✉ [jia.liu@siat.ac.cn](mailto:jia.liu@siat.ac.cn))

Shenzhen Institutes of Advanced Technology Chinese Academy of Sciences

**Zhijun Zhang** (✉ [janemengzhang@vip.163.com](mailto:janemengzhang@vip.163.com))

Southeast University <https://orcid.org/0000-0001-5480-0888>

**Keywords:** Computational fluid dynamics, Hemodynamics, Cerebral blood flow, Cerebrovascular resistance, Alzheimer's disease

**Posted Date:** June 7th, 2020

**DOI:** <https://doi.org/10.21203/rs.3.rs-32881/v1>

**License:** © ⓘ This work is licensed under a Creative Commons Attribution 4.0 International License.

[Read Full License](#)

---

1 Using hemodynamic parameters quantified with computational fluid  
2 dynamics to explore potential mechanisms of occurrence and progression  
3 in Alzheimer Disease

4 Jian Xie<sup>§1</sup>, Zaiheng Cheng<sup>§2</sup>, LiHua Gu<sup>1</sup>, Bokai Wu<sup>2</sup>, Gao-jia Zhang<sup>3</sup>, Wen-Shin Shiu<sup>2</sup>, ,  
5 Rongliang Chen<sup>2</sup>, Zan Wang<sup>1</sup>, Chang Liu<sup>2</sup>, Xiao-chuan Cai<sup>4</sup>, Li-Ping Wang<sup>2</sup>, Jia Liu<sup>\*2</sup>,  
6 Zhijun Zhang<sup>1\*</sup>

7 § These authors contributed equally to this work.

8 \*Correspondence: [janemengzhang@vip.163.com](mailto:janemengzhang@vip.163.com); [jia.liu@siat.ac.cn](mailto:jia.liu@siat.ac.cn).

9 <sup>1</sup>Zhijun Zhang, PhD& MD, Department of Neurology, Affiliated ZhongDa Hospital,  
10 School of Medicine , Southeast University , Nanjing , Jiangsu 210009 , China.

11 <sup>2</sup>Jia Liu, PhD, Shenzhen Institutes of Advanced Technology, Chinese Academy of  
12 Sciences, Shenzhen, Guangzhou 518055, China.

13 Full list of author information is available at the end of the article

14 **Abstract**

15 **Background:** It has gradually recognized that the patients with Alzheimer's disease  
16 (AD) have cerebral hemodynamic disorders. The purpose of the present study was to  
17 exploit a novel computational fluid dynamics (CFD) model, which could be used to  
18 measure intracranial hemodynamics quantitatively in AD patients and to further explore  
19 how the hemodynamic changes are involved in progression of AD.

20 **Methods:** A novel CFD model was constructed by personal magnetic resonance  
21 angiography (MRA), vessel ultrasound and blood pressure value of all subjects, of  
22 whom included AD patients, vascular dementia (VaD) patients and well-matched

23 healthy controls (HCs). Demographic, clinical and imaging data of all subjects were  
24 recorded and analyzed. Quantitative total cerebral blood flow (CBF) and  
25 cerebrovascular resistance (CVR) were compared among three groups, in order to  
26 ascertain the potential hemodynamic disorders in AD patients.

27 **Results:** Total CBF and CVR of AD patients were significantly different from those of  
28 HCs (both  $P<0.01$ ), but not different from patients with VaD (both  $P>0.5$ ), despite the  
29 cerebral arteries in AD patients were anatomically intact. Total CBF was negatively  
30 correlated with total CVR ( $r_s=-0.822$ ,  $P<0.001$ ) in AD patients. Comparing with HCs,  
31 Elevated CVR ( $OR=2.25$ ,  $P=0.004$ ) and age ( $OR=2.06$ ,  $P=0.021$ ) were independent  
32 risk factor of AD.

33 **Conclusions:** CFD can be applied to non-invasively and conveniently quantify and  
34 visualize biomechanical changes of cerebral blood flow. Patients with AD have  
35 dysfunction of cerebral hemodynamic, including lower CBF and higher CVR, and the  
36 CVR was an independent risk factor of AD. These findings provide quantitative  
37 evidence to support that increase of cerebrovascular resistance may involve in  
38 development of AD.

39 **Key words:** Computational fluid dynamics, Hemodynamics, Cerebral blood flow,  
40 Cerebrovascular resistance, Alzheimer's disease.

#### 41 **Introduction**

42 Dementia is a disorder characterized by the impairment of cognitive function with  
43 attenuated daily activity and psychiatric symptoms. Dementia is the third contributor of  
44 neurological disability-adjusted life-years (DALYs) <sup>[1]</sup>. More than 50 million people are

45 affected by the dementia globally, it has been estimated that the total number of  
46 dementia patients worldwide will reach 76 million by 2030 and 135 million by 2050<sup>[2]</sup>.  
47 AD and VaD are the most common causes of dementia<sup>[3]</sup>. As acknowledged by  
48 clinicians, lifestyle and vascular risk factors accelerate VaD progression<sup>[4]</sup>. However,  
49 recently studies indicated that cardiovascular risk factors correlate with the occurrence  
50 and development of AD<sup>[5]</sup>. For example, previous studies have confirmed higher  
51 vascular risk and lower physical activity are associated with burden of  $\beta$ -Amyloid and  
52 cognitive decline<sup>[6, 7]</sup>.

53 The circulatory pathophysiological changes mediated by vascular risk factors were  
54 always accompanied by intracranial hemodynamic disorder, which was involved in  
55 mechanisms of cognitive decline<sup>[5-7]</sup>. For instance, patients with cardiac dysfunction  
56 manifest hemodynamic disorders and decreased cerebral perfusion, which subsequently  
57 lead to injury or death of neurons<sup>[8, 9]</sup>. Moreover, remodeling and cerebral vasomotor  
58 disorders of intracranial or extracranial vessels reduce cerebral perfusion and increase  
59 resistance of cerebral arteries, which impair metabolism of nervous tissue and clearance  
60 of A- $\beta$  amyloid, further exacerbate cognitive decline<sup>[10-12]</sup>. Therefore detection of  
61 hemodynamic disorders may contribute to identification potentially pathophysiological  
62 changes in dementia patients.

63 Hemodynamic parameters can be measured indirectly through some medical  
64 imaging techniques, including arterial spin labeling (ASL) MRI, transcranial doppler  
65 ultrasonography (TCD), oxygen-15-labelled water positron emission tomography  
66 (PET), four dimensional (4D) flow MRI. Using ASL, the CBF ratio of gray

67 matter/white matter has been shown to decline globally in the poststroke dementia  
68 patients<sup>[13]</sup>, AD patients also exhibit increased CVR index (CVRi) and diminished CBF  
69 in inferior parietal and temporal cerebral<sup>[14, 15]</sup>. However, ASL has poor noise to signal  
70 ratio and only reflects changes in a small portion of hemodynamic parameters. Flow  
71 velocity and the pulsatility index can be evaluated by TCD, in which, increased CVRi  
72 were found in aged adults<sup>[16]</sup> and AD patients <sup>[17]</sup>. A meta-analysis indicated that  
73 hemodynamic disturbance in VaD was more severe than that of AD<sup>[18]</sup> . However, TCD  
74 cannot accurately detect hemodynamic parameters of distal arterial branches,  
75 furthermore, the accuracy of TCD relies on an experienced operator and interpreter.  
76 PET only measures the CBF and is applied limitedly. The 4D flow MRI is an emerging  
77 imaging paradigm and capable to quantify the temporal evolution of complex blood  
78 flow patterns within an acquired 3D volume, by which AD patients have been found to  
79 have decreased mean flow in the internal carotid and middle cerebral arteries <sup>[19]</sup>.  
80 However, there is a trade-off between the spatial and temporal resolution of 4D-flow  
81 MRI, it is suitable either for the large arteries with fast velocity or the narrow vessels  
82 with slow velocity, such as measurements of blood flow velocity in the aorta or veins,  
83 thereby limiting the applications of 4D-flow MRI in cerebral arteries.

84 CFD is a well-established technique that provides comprehensive information of  
85 hemodynamics non-invasively. Various 3D CFD models using routinely available  
86 medical imaging had been proposed and applied to evaluate hemodynamic parameters,  
87 for example, fractional flow reserve (FFR) was calculated by CFD based on computed  
88 tomography angiography (CTA) , which has been approved to assess the risk of

89 coronary stenosis, and CFD derived FFR is highly comparable with the FFR measured  
90 by a interventional pressure wire<sup>[20, 21]</sup>. CFD technique can reduce unnecessary  
91 interventional angiography effectively and help doctors to diagnose pathological  
92 conditions<sup>[22, 23]</sup>. Moreover, CFD can be applied to assess the risk of rupture and  
93 pressure of the intracranial aneurysm, thereby improving the understanding of the  
94 biomechanics of the aneurysms<sup>[24]</sup>.

95 To our knowledge, there is lack of study on hemodynamic alterations in AD patients  
96 using CFD. The present study would use self-constructed CFD model to quantify the  
97 hemodynamic parameters and compared among three groups: (1) AD patients, (2) VaD  
98 patients as positive controls and (3) HCs as negative controls, so as to explore potential  
99 mechanisms of occurrence and progression in Alzheimer Disease.

## 100 **Methods**

### 101 **Participants**

102 The present cross-sectional study included AD patients (n=30), VaD patients  
103 (n=29), and HCs (n=34). Probable AD diagnosis was determined in accordance with  
104 the criteria of the National Institute of Neurological and Communicative Disorders and  
105 Stroke, and the AD and Related Disorders Association (NINCDS-ADRDA). Probable  
106 VaD was diagnosed in accordance with the criteria of the International Classification of  
107 Diseases-10 (ICD-10). Individuals who were cognitively normal were also included to  
108 be HCs. All participants received MRI+MRA and ultrasound of cervical arteries.

109 Subjects were excluded from the study if they suffered from heavy organ dysfunction,  
110 or a history of cognitive disorders. The study was approved by the ethics committee of

111 the affiliated ZhongDa hospital of Southeast University.

## 112 **Collection of demographic data**

113 All participants underwent comprehensive medical and neurological evaluations,  
114 fasting venous blood samples were collected for routine blood testing and blood  
115 biochemical parameters (Table 1 and Supplementary Table S1). The 10-year risk of  
116 heart disease or stroke was determined using the ASCVD algorithm (website:  
117 <http://www.cvriskcalculator.com/>), which was used to evaluate the risk factor burden  
118 of cardiovascular and cerebrovascular diseases, ASCVD scores were categorized as low,  
119 moderate and high risk depending on the risk stratification. Mean arterial pressure  
120 (MAP) was calculated by formula:  $MAP = DBP + (SBP - DBP) / 3$ .

## 121 **Protocols of imaging**

122 The systolic and diastolic BP of participant were measured prior to examination  
123 of cervical vessel ultrasound in the same morning. Doppler ultrasonography was  
124 performed to measure velocities of the left and right internal carotid and vertebral  
125 arteries (CCA/VA) using high-resolution ultrasound (GE, LOGIQ E9) at 8-15 MHz, in  
126 which, peak systolic velocity (PSV) and end diastolic velocity (EDV) acted as two  
127 important indexes to build CFD model. All patients were scanned using a 3T clinical  
128 MRI system (Siemens) with a 12-channel head and neck coil array. The MR scan  
129 included parenchymal brain imaging sequences (axial DWI, T2 FLAIR, and T1), MRA  
130 was performed on axial 3D TOF MRA (TR = 15.0 ms, TE = 3.45 ms, flip angle = 25,  
131 NEX = 1, field of view = 242 x 242 mm, matrix size 512 x 512, 24 slices x 3 sections,  
132 slice thickness 1 mm).

## 133 **Hemodynamic measurement of subjects using CFD**

### 134 *Image processing and CFD mesh generation*

135 MRA images were exported from computing the server of the MRI scanner in  
136 standard Digital Imaging and Communication in Medicine (DICOM) format. The  
137 cerebral artery was segmented from each DICOM image using 3D region-growing  
138 provided by Mimics (Materialise NV, Belgium), in which results were inspected and  
139 refined by two radiologists. The 3D surface of the cerebral artery was then reconstructed.  
140 The computational domain of CFD was defined by a mesh generated by ANSYS ICEM  
141 CFD software (ANSYS, Inc., USA). Due to the complexity of the geometry, an  
142 unstructured tetrahedral cell was used for domain discretization. The total number of  
143 elements was greater than 1 million with a minimum volume of approximately  $1.0 \cdot 10^{-8}$   
144  $\text{cm}^3$  in order to capture features of flow dynamics in small-scale, to provide more  
145 detailed computation of the hemodynamics, especially within the stenotic artery.

### 146 *Modelling of blood flow in 3D*

147 The blood flow was assumed to be a viscous and incompressible Newtonian fluid,  
148 the heat transfer and compressibility effects of the vascular wall were neglected in this  
149 process. The blood flow were defined as a constant density  $\rho = 1.06 \times 10^3 \text{kg} \cdot \text{m}^{-3}$   
150 and dynamic viscosity  $\mu = 3.5 \times 10^{-3} \text{kg} \cdot \text{m}^{-1} \cdot \text{s}^{-1}$ , as the simulated blood flow was  
151 not sensitive to these parameters<sup>[25, 26]</sup>. A typical carotid artery diameter  $D =$   
152  $6.0 \times 10^{-3} \text{m}$  and its corresponding velocity of blood flow  $v = 0.4 \text{m} \cdot \text{s}^{-1}$  were  
153 assumed in order to calculate the Reynolds number:  $Re = \rho v D / \mu \approx 121$ , which  
154 suggested that the blood flow was laminar. A 3D unsteady incompressible Navier-

155 Stokes equation was then utilized to describe the blood flow, as follows:

$$156 \quad \rho \frac{\partial \mathbf{v}}{\partial t} + (\mathbf{v} \cdot \nabla) \mathbf{v} = -\nabla p + \mu \nabla^2 \mathbf{v} + \mathbf{f}, \quad (1.1)$$

157 The equation for conservation of mass was defined as:

$$158 \quad \nabla \cdot \mathbf{v} = 0, \quad (1.2)$$

159 where  $\mathbf{v}$  was the velocity vector,  $p$  was the pressure, and  $\mathbf{f}$  was force of the body,  
160 assumed equal to 0.

161 To solve equations (1.1) and (1.2), a finite volume approach using ANSYS CFX  
162 software version 14.5 (ANSYS, Inc., USA) was used. CFD simulations were conducted  
163 on an AMAX server with dual 22-core Intel Xeon E5-2699 v4 CPUs running at  
164 2.20GHz with 256GB memory. Mesh partitioning was performed using a k-way Metis  
165 algorithm with a message passing interface (MPI) unutilized for multi-core  
166 communication. A five second period of blood flow in each cerebral artery was  
167 simulated with a time step of 0.01 s. A second-order backward Euler scheme was used  
168 for the transient term. The criteria for convergence was set at a root mean square error  
169 (RMSE) for the relative levels of  $1.0 \times 10^{-5}$ .

### 170 ***Determination of Boundary conditions***

171 Both PSV and EDV at each internal carotid artery (ICA) and vertebral artery (VA)  
172 were used as the inlet boundary conditions to estimate the respective mean velocities,  
173 as  $V_{mean} = \frac{1}{3}V_{PSV} + \frac{2}{3}V_{EDV}$ . The mean velocities were assumed to be present at the  
174 centerline of the vessels, the flow was further assumed to be laminar with pulsatility  
175 neglected at all inlets. Inlet blood flow was then approximated by  $Q_{in} = \frac{1}{2}V_{mean} \cdot A_{in}$ ,

176 where  $A_{in}$  represents the cross-sectional area of the artery at the inlet, as the  
177 hemodynamic assumption resulted in a Poiseuille velocity profile, which is parabolic<sup>[27]</sup>.  
178 The cross-sectional area was calculated by  $A_{in} = \pi \cdot (\frac{D_{in}}{2})^2$ , where  $D_{in}$  was the  
179 diameter of the inlet artery, measured from the MRA images. Total CBF was  
180 preliminarily obtained from the sum of internal carotid and vertebral  $Q_{in}$ . For the outlet  
181 boundary conditions, pressure  $P_{out}$  was estimated at each outlet. A resistive boundary  
182 condition was applied to each outlet of the distal artery to mimic the downstream  
183 resistance, assumed to be inversely proportional to the diameter of the outlet. In order  
184 to achieve this, total CVR  $R_{total}$  was calculated from the total inflow  $Q_{total} =$   
185  $Q_{in}^{ICA} + Q_{in}^{VA}$  and mean arterial pressure (MAP), approximated by brachial blood  
186 pressure. Initial  $R_{total}$  was then calculated from  $R_{total} = MAP/Q_{total}$ .  $R_{out}$  at each  
187 outlet was estimated from  $R_{total}$  depending on the diameter of the outlet ( $D_{out}$ ) as  
188 calculated from MRA images. Finally, the outlet pressure  $P_{out}$  was calculated by  
189  $P_{out} = Q_{out} \cdot R_{out}$ , where  $Q_{out}$  was the flow rate at each outlet, estimated from the  
190 integral of the outlet velocity  $V_{out}$  at the outlet area.

### 191 **Statistical analysis**

192 Statistical analyses were performed using SPSS version 25.0 (IBM Corp.).  
193 Normality of continuous data was confirmed using a Shapiro-Wilk test, and  
194 homogeneity of variance assessed using Levene test. Data are presented as means  $\pm$   
195 standard deviation (SD). Categorical data are expressed numerically. Analysis of  
196 differences in demographic, clinical characteristics, and CFD among the three groups  
197 were conducted using a one-way analysis of variance (ANOVA), and Kruskal-Wallis

198 test or  $\chi^2$  test. Where a significant difference was found, Dunnett's, Pairwise  
199 Comparisons and Bonferroni methods were used to adjust for each two groups  
200 respectively. Differences in CBF or CVR between gender, with or without a history of  
201 stroke were analyzed by independent sample t tests and Kruskal-Wallis test  
202 respectively. The correlation between CBF, CVR and age were explored using  
203 Spearman correlation analyses. To elucidate the independent contributions of  
204 hemodynamic parameters to dementia, binary logistic regression analyses were  
205 performed for patients and HCs groups, statistically significant independent variables  
206 in univariate analysis were included in a binary regression. In these analyses, AD or  
207 VaD was the dependent variable, gender, age, history of stroke, CBF and CVR were  
208 independent variables. According to the interquartile range of all subjects, CBF and  
209 CVR were divided into four continuous levels (supplementary Table 2), with entry and  
210 removal criteria of 0.05 and 0.1, respectively. For significant findings, odds ratios (*OR*)  
211 were calculated to interpret the effect on "dementia". *P*-values of <0.05 were  
212 considered statistically significant.

## 213 **Results**

### 214 **Comparison of baseline demographic and clinical characteristics among three** 215 **groups**

216 The baseline demographic and clinical characteristics are summarized in Table1  
217 for the three groups. There were significant differences in age ( $F=14.713$ ,  $P<0.001$ ),  
218 gender distribution( $\chi^2 =13.449$ ,  $P=0.001$ ) and percentage of stroke history ( $\chi^2=12.041$ ;  
219  $P=0.002$ ) among three groups. As compared to HCs, average age of VaD patients

220 ( $P<0.001$ ) and AD patients ( $P=0.005$ ) were older than HCs, however, no significant  
221 difference for age was founded between AD and VaD patients ( $P=0.058$ ). As compared  
222 with AD and HCs groups, the proportion of male and history of stroke in VaD group  
223 were significantly increased (both  $P<0.05$ ). Additional information for all subjects is  
224 displayed in Supplementary Table S1.

### 225 **Comparison of Hemodynamic parameters among groups**

226 Three typical color maps of pressure and velocity throughout the arterial tree are  
227 displayed in Figure 1 for three subjects: AD (a, b), VaD (c, d), and HCs (e, f). Both AD  
228 and VaD patients had diminished blood supply even if the arterial trees of AD patient  
229 were anatomically intact. CBF and CVR in arteries that were larger than 0.2cm in  
230 diameter could be estimated by the CFD model (Supplementary figure S1). The  
231 hemodynamic parameters of all subjects were calculated by the 3D CFD model (Table  
232 2). As compared with HCs, there were significant reduced total CBF or increased total  
233 CVR in AD group (CBF:  $P=0.008$ ; CVR:  $P=0.009$ ) and VaD group (CBF:  $P=0.002$ ;  
234 CVR:  $P=0.001$ ), however no significant difference in the CBF and CVR were founded  
235 between AD and VaD patients (CBF:  $P=0.905$ ; CVR:  $P=0.524$ ). Other hemodynamic  
236 parameters of all subjects are displayed in Supplementary Table S2

237 Figure 1 Three typical examples of pressure distribution and stream lines of blood flow velocity are  
238 displayed in the first and the second row, respectively. The first column (fig a and b) is for an AD  
239 patients, the second column (fig c and d) is for a VaD patients, and the third column (fig e and f) is  
240 for a healthy subject. It is evident that the AD patient and the healthy subject are with intact arterial  
241 trees, whereas VaD the patient is with scarce arterial branches. However, according to computation,

242 the total blood flow in the models was 692 ml/min (AD patient), 647 ml/min (VaD patient), and 998  
243 ml/min (healthy subject) respectively.

#### 244 **Interactive associations of the hemodynamic parameters and risk factors**

245 Bivariate Spearman correlation showed that total CBF was negatively correlated  
246 with total CVR in whole subjects (fig 2a,  $r_s=-0.826$ ,  $P<0.001$ ) and AD groups(fig 2b,  
247  $r_s=-0.822$ ,  $P<0.001$ ). There were significant correlations between age and total CBF  
248 (fig 2c,  $r_s=-0.282$ ,  $P<0.05$ ) or total CVR(fig 2d,  $r_s=0.278$ ,  $P<0.05$ ), however there was  
249 no significant difference in total CVR (fig 2e,  $Z=-0.968$ ;  $P=0.333$ ) or CBF(fig 2f,  
250  $t=0.759$ ;  $P=0.450$ ) between male and female subjects. Meanwhile, as compared with  
251 subjects without past history of stroke, the subjects with history of stroke have a higher  
252 total CVR (fig 2g,  $Z=-2.179$ ;  $P=0.029$ ), but not CBF (fig 2h,  $t=1.793$ ;  $P=0.076$ ).

253 **Figure 2** Interactive associations of the hemodynamic parameters and risk factors, correlation  
254 between total CBF and CVR in all subjects (a) and AD group(b), (c) and (d) showed significant  
255 correlations between CBF or CVR and age, fig(e, f) showed there were no significant difference of  
256 total CVR or CBF between male and female patients, fig(g) indicated there was significant  
257 difference of total CVR in patients with stroke or not, but not total CBF fig(h).ns: no significance,  
258 \* $P<0.05$ .

#### 259 **Association between hemodynamic parameters and dementia**

260 Binary regression demonstrated that age (10-year increment;  $P=0.021$ ) and CVR  
261 ( $P=0.004$ ) were independent risk factors for AD (Table 3). Independent risk factors of  
262 VaD included age (10-year increment;  $P=0.001$ ), gender ( $P=0.014$ )and CVR ( $P=0.033$ ).

#### 263 **Discussion**

264 This present study exploited a 3-D CFD model to quantitatively measure the  
265 changes of CBF and CVR in AD patients for the first time. The main findings are  
266 summarized as follows. Firstly, as compared with HCs, both total CBF and CVR in AD  
267 or VaD groups were significantly changed, no differences were observed in total CBF  
268 and CVR between AD and VaD groups. Secondly, total CBF was negatively correlated  
269 with CVR in all subjects. Finally, elevated CVR and age associated with increased risk  
270 of AD, suggesting that changed cerebral hemodynamic are present in AD patients.

271 It is challenging to measure hemodynamics directly. Previous studies have used  
272 other methods to non-invasively quantify the CBF and CVR<sup>[15, 28-31]</sup>. In current study, a  
273 CFD model was constructed individually by the subject-specific medical images, It is  
274 non-invasive and not limited by contraindications of imaging examinations , CTA and  
275 DSA data can also be used to replace MRA, hence it is accessible to most medical  
276 centers. The model has high spatial resolution, and arteries with diameter larger than  
277 0.2cm can be evaluated, allowing hemodynamic parameters even in the distal branches  
278 to be available. Furthermore, comprehensive hemodynamic parameters, such as CBF,  
279 velocity, CVR, FFR, and arterial wall shear stress can be acquired anywhere of the  
280 artery conveniently in the 3D model.

281 During undertaking cognitive task, healthy subjects and stroke patients exhibited  
282 a significant increase both in CBF and blood stream velocity<sup>[10, 32]</sup>, which suggested  
283 that cerebrovascular circulation adjusts its hemodynamic response to metabolic  
284 requirements. However, the total CBF of the internal carotid and vertebral arteries were  
285 decreased in VaD patients<sup>[28]</sup>, Furthermore, a marked decreased CBF in the parietal and

286 frontal cortex of AD or VaD patients has been observed, which was associated with  
287 increased subcortical white matter lesions in VaD patients<sup>[33]</sup>. Stabilized CBF is  
288 dependent on heart function and resistance of intracranial vessels<sup>[9]</sup>, the CVRi of  
289 middle cerebral arteries<sup>[17]</sup>, cortex and subcortex were increased in AD patients,  
290 particularly within the thalamus and caudate<sup>[16, 34]</sup>. In addition CVRi was positively  
291 correlated with severity of dementia<sup>[17]</sup>. Hence hemodynamic alterations were involved  
292 in the pathophysiology of AD, therefore the alterations of vascular resistance may play  
293 an important role progression of AD and VaD.

294       However previous studies only analyzed the correlation between AD and CVR or  
295 CBF respectively. In present study, the decreased total CBF and increased CVR were  
296 observed in AD group, and total CVR was an independent risk factor of AD, more  
297 importantly, the total CBF was significantly and negatively correlated with total CVR.  
298 Therefore, the CBF may be regulated by CVR. All above results demonstrated that the  
299 increase of vascular resistance may affect the perfusion of whole brain and occurrence  
300 of AD. Therefore, early discovery of changes in CVR indicates that potential  
301 cerebrovascular lesions in AD.

302       The increases of cerebral resistance in AD patients are caused by other potential  
303 mechanisms. Recent research confirmed that capillary constriction caused by A $\beta$   
304 induces energy lack and neurodegeneration in neuron<sup>[35]</sup>, which subsequently elevate  
305 the cerebral vascular resistance. Moreover the cerebral vascular resistance may be  
306 increased by mixed brain lesions and remodeling of cerebral microvasculature which  
307 were mediated by vascular risk factors<sup>[6, 7]</sup>. Consequently the treatments of AD should

308 include the alleviation of cerebrovascular lesions, careful control or decreased exposure  
309 to risk factors may attenuate cognitive decline, and alleviation of the capillary  
310 contraction caused by A $\beta$  may be a new treatment direction of AD.

### 311 **Limitations**

312 There are some limitations to this study. Firstly, it is a cross-sectional research  
313 study, the correlation between hemodynamic parameters and AD need to be verified by  
314 follow-up studies. In a future study we will verify the correlation between more  
315 hemodynamic parameters and dementia with follow-up investigation, in addition the  
316 effect of hemodynamics on progression. Secondly, the diagnosis of AD was based on  
317 clinical data and lack of neuropathic markers. Thirdly, due to the small number of  
318 patients, which may restrict findings of this study, and the large-scale clinical studies  
319 were needed for further verified. Finally, the sensitivity and specificity of CFD require  
320 comparison with other non-invasive methods to explore the practicality of CFD.

### 321 **Conclusions**

322 CFD can be used to distinguish hemodynamic changes between AD patients and  
323 healthy subjects. AD patients had lower CBF and higher CVR, and the CVR was an  
324 independent risk factor of AD, Early detection of alterations of CVR will help clinicians  
325 find potential cerebrovascular lesions, alleviation of CVR may be another direction of  
326 treatment in AD.

### 327 **Supplementary information**

328 Table S1. Supplementary demographics and clinical characteristics of all subjects.

329 Table S2. Hemodynamic parameters of all subjects. FigureS1. Procedure of CFD model.

330 **Abbreviations**

331 AD: Alzheimer’s disease, ASL: arterial spin labeling, BMI: body mass index, CFD:  
332 computational fluid dynamics, CVR: cerebral vascular resistance, CVRi: CVR index,  
333 CBF: cerebral blood flow, CHD: coronary heart disease, DBP: diastolic blood pressure,  
334 EDV: end diastolic velocity, FFR: fractional flow reserve, GT: triglycerides, HCs:  
335 healthy control subjects, HDL: high-density lipoprotein, Hb: hemoglobin, LDL: low-  
336 density lipoprotein, MAP: mean arterial pressure, MRA: magnetic resonance  
337 angiography, PSV: peak systolic velocity, SBP: systolic BP, Tc: total cholesterol, TCD:  
338 transcranial doppler ultrasonography, VaD: vascular dementia.

339 **Acknowledgements**

340 We wish to thank all participants in this study, without whose agreement this research  
341 would not have been possible. We thank the colleagues who participated in the  
342 collection of the clinical data.

343 **Author’s contributions**

344 ZJZ and JL designed the study, analyzed and interpreted of data, and drafted and revised  
345 the manuscript, JL Jia contributed to technique writing. JX collected, analyzed and  
346 interpreted the data, prepared all statistic figures, drafted the manuscript. ZC and BW  
347 contributed to arterial 3D reconstruction and mesh generation. GJZ, GLH and ZW  
348 contributed to collected the clinical data, WSS, RLC and XCC contributed to numerical  
349 computation, CL contributed to medical image processing, LPW participated in design  
350 the study. All authors contributed to the writing and revisions of the paper and approved  
351 the final version.

352 **Funding**

353 This research was supported by grants from the National Natural Science Foundation  
354 of China (81420108012, 81671046 to Z.Z.), Program of Excellent Talents in Medical  
355 Science of Jiangsu Province (JCRCA2016006 to Z.Z.). National Natural Science  
356 Foundation of China (81661168015, 61703017, 81871447 to JL), and Shenzhen  
357 Science and Technology Innovation Commission (ZDSYS201703031711426 to JL).  
358 The funding bodies had no role in the design of the study, data collection, ana-lysis,  
359 interpretation, or writing of the manuscript.

360 **Availability of data and materials**

361 The dataset used during the current study is available from the corresponding author on  
362 reasonable request.

363 **Ethics approval and consent to participate**

364 The study was approved by the Institutional Ethical Committee of Nanjing ZhongDa  
365 Hospital, Southeast University and the participants gave written informed consents  
366 prior to obtain the data.

367 **Consent for publication**

368 Not applicable

369 **Competing interests**

370 The authors declare that they have no competing interests.

371 **Author details**

372 <sup>1</sup>Department of Neurology, Affiliated ZhongDa Hospital, School of Medicine,  
373 Southeast University, Nanjing, Jiangsu 210009, China.<sup>2</sup>Shenzhen Institutes of

374 Advanced Technology, Chinese Academy of Sciences.<sup>3</sup>Department of Neurology,  
375 Nanjing Lishui people's Hospital, Nanjing, China.<sup>4</sup>Department of Computer Science,  
376 University of Colorado Boulder.

377

## 378 **References**

- 379 1. Collaborators GBDN. Global, regional, and national burden of neurological disorders, 1990-2016:  
380 a systematic analysis for the Global Burden of Disease Study 2016. *Lancet Neurol.* 2019;18(5):459-80.
- 381 2. International AsD. World Alzheimer Report 2018 2018.
- 382 3. O'Brien JT, Thomas A. Vascular dementia. *Lancet.* 2015;386(10004):1698-706.
- 383 4. Larsson SC, Markus HS. Does Treating Vascular Risk Factors Prevent Dementia and Alzheimer's  
384 Disease? A Systematic Review and Meta-Analysis. *J Alzheimers Dis.* 2018;64(2):657-68.
- 385 5. Philip Scheltens KB, Monique M B Breteler, Bart de Strooper, Giovanni B Frisoni, Stephen  
386 Salloway, Wiesje Maria Van der Flier. Alzheimer's disease. *Lancet* 2016(388):505-17.
- 387 6. Rabin JS, Klein H, Kirn DR, Schultz AP, Yang HS, Hampton O, et al. Associations of Physical  
388 Activity and beta-Amyloid With Longitudinal Cognition and Neurodegeneration in Clinically Normal  
389 Older Adults. *JAMA Neurol.* 2019.
- 390 7. Wang R, Fratiglioni L, Kalpouzos G, Lovden M, Laukka EJ, Bronge L, et al. Mixed brain lesions  
391 mediate the association between cardiovascular risk burden and cognitive decline in old age: A  
392 population-based study. *Alzheimers Dement.* 2017;13(3):247-56.
- 393 8. Stewart RAH, Held C, Krug-Gourley S, Waterworth D, Stebbins A, Chiswell K, et al.  
394 Cardiovascular and Lifestyle Risk Factors and Cognitive Function in Patients With Stable Coronary  
395 Heart Disease. *J Am Heart Assoc.* 2019;8(7):e010641.

- 396 9. van der Velpen IF, Feleus S, Bertens AS, Sabayan B. Hemodynamic and serum cardiac markers  
397 and risk of cognitive impairment and dementia. *Alzheimers Dement.* 2017;13(4):441-53.
- 398 10. Heffernan KS, Augustine JA, Lefferts WK, Spartano NL, Hughes WE, Jorgensen RS, et al.  
399 Arterial stiffness and cerebral hemodynamic pulsatility during cognitive engagement in younger and  
400 older adults. *Exp Gerontol.* 2018;101:54-62.
- 401 11. Buratti L, Viticchi G, Falsetti L, Balucani C, Altamura C, Petrelli C, et al. Thresholds of impaired  
402 cerebral hemodynamics that predict short-term cognitive decline in asymptomatic carotid stenosis.  
403 *Journal of cerebral blood flow and metabolism : official journal of the International Society of Cerebral  
404 Blood Flow and Metabolism.* 2016;36(10):1804-12.
- 405 12. Nielsen RB, Egefjord L, Angleys H, Mouridsen K, Gejl M, Moller A, et al. Capillary dysfunction  
406 is associated with symptom severity and neurodegeneration in Alzheimer's disease. *Alzheimers  
407 Dement.* 2017;13(10):1143-53.
- 408 13. Kim CM, Alvarado RL, Stephens K, Wey HY, Wang DJJ, Leritz EC, et al. Associations between  
409 cerebral blood flow and structural and functional brain imaging measures in individuals with  
410 neuropsychologically defined mild cognitive impairment. *Neurobiol Aging.* 2019.
- 411 14. Yew B, Nation DA, Alzheimer's Disease Neuroimaging I. Cerebrovascular resistance: effects on  
412 cognitive decline, cortical atrophy, and progression to dementia. *Brain.* 2017;140(7):1987-2001.
- 413 15. Firbank MJ, He J, Blamire AM, Singh B, Danson P, Kalaria RN, et al. Cerebral blood flow by  
414 arterial spin labeling in poststroke dementia. *Neurology.* 2011;76(17):1478-84.
- 415 16. Clark LR, Nation DA, Wierenga CE, Bangen KJ, Dev SI, Shin DD, et al. Elevated  
416 cerebrovascular resistance index is associated with cognitive dysfunction in the very-old. *Alzheimers  
417 Res Ther.* 2015;7(1):3.

- 418 17. Gommer ED, Martens EG, Aalten P, Shijaku E, Verhey FR, Mess WH, et al. Dynamic cerebral  
419 autoregulation in subjects with Alzheimer's disease, mild cognitive impairment, and controls: evidence  
420 for increased peripheral vascular resistance with possible predictive value. *J Alzheimers Dis.*  
421 2012;30(4):805-13.
- 422 18. Sabayan B, Jansen S, Oleksik AM, van Osch MJ, van Buchem MA, van Vliet P, et al.  
423 Cerebrovascular hemodynamics in Alzheimer's disease and vascular dementia: a meta-analysis of  
424 transcranial Doppler studies. *Ageing Res Rev.* 2012;11(2):271-7.
- 425 19. Berman SE, Clark LR, Rivera-Rivera LA, Norton D, Racine AM, Rowley HA, et al. Intracranial  
426 Arterial 4D Flow in Individuals with Mild Cognitive Impairment is Associated with Cognitive  
427 Performance and Amyloid Positivity. *J Alzheimers Dis.* 2017;60(1):243-52.
- 428 20. Min JK, Leipsic J, Pencina MJ, Berman DS, Koo BK, van Mieghem C, et al. Diagnostic accuracy  
429 of fractional flow reserve from anatomic CT angiography. *JAMA.* 2012;308(12):1237-45.
- 430 21. Ko BS, Wong DT, Norgaard BL, Leong DP, Cameron JD, Gaur S, et al. Diagnostic Performance  
431 of Transluminal Attenuation Gradient and Noninvasive Fractional Flow Reserve Derived from 320-  
432 Detector Row CT Angiography to Diagnose Hemodynamically Significant Coronary Stenosis: An NXT  
433 Substudy. *Radiology.* 2016;279(1):75-83.
- 434 22. Taylor CA, Fonte TA, Min JK. Computational fluid dynamics applied to cardiac computed  
435 tomography for noninvasive quantification of fractional flow reserve: scientific basis. *J Am Coll*  
436 *Cardiol.* 2013;61(22):2233-41.
- 437 23. Randles A, Frakes DH, Leopold JA. Computational Fluid Dynamics and Additive Manufacturing  
438 to Diagnose and Treat Cardiovascular Disease. *Trends in biotechnology.* 2017;35(11):1049-61.
- 439 24. Saqr KM, Rashad S, Tupin S, Niizuma K, Hassan T, Tominaga T, et al. What does computational

440 fluid dynamics tell us about intracranial aneurysms? A meta-analysis and critical review. *Journal of*  
441 *cerebral blood flow and metabolism : official journal of the International Society of Cerebral Blood*  
442 *Flow and Metabolism*. 2019;271678x19854640.

443 25. Nam HS, Scalzo F, Leng X, Ip HL, Lee HS, Fan F, et al. Hemodynamic Impact of Systolic Blood  
444 Pressure and Hematocrit Calculated by Computational Fluid Dynamics in Patients with Intracranial  
445 Atherosclerosis. *J Neuroimaging*. 2016;26(3):331-8.

446 26. Arzani A. Accounting for residence-time in blood rheology models: do we really need non-  
447 Newtonian blood flow modelling in large arteries? *J R Soc Interface*. 2018;15(146).

448 27. Mynard JP, Steinman DA. Effect of velocity profile skewing on blood velocity and volume flow  
449 waveforms derived from maximum Doppler spectral velocity. *Ultrasound Med Biol*. 2013;39(5):870-  
450 81.

451 28. Scheel P, Puls I, Becker G, Schoning M. Volume reduction in cerebral blood flow in patients with  
452 vascular dementia. *Lancet*. 1999;354(9196):2137.

453 29. Mazzucco S, Li L, Tuna MA, Pendlebury ST, Wharton R, Rothwell PM, et al. Hemodynamic  
454 correlates of transient cognitive impairment after transient ischemic attack and minor stroke: A  
455 transcranial Doppler study. *Int J Stroke*. 2016;11(9):978-86.

456 30. Rivera-Rivera LA, Schubert T, Turski P, Johnson KM, Berman SE, Rowley HA, et al. Changes in  
457 intracranial venous blood flow and pulsatility in Alzheimer's disease: A 4D flow MRI study. *Journal of*  
458 *cerebral blood flow and metabolism : official journal of the International Society of Cerebral Blood*  
459 *Flow and Metabolism*. 2017;37(6):2149-58.

460 31. Binnewijzend MA, Kuijter JP, Benedictus MR, van der Flier WM, Wink AM, Wattjes MP, et al.  
461 Cerebral blood flow measured with 3D pseudocontinuous arterial spin-labeling MR imaging in

462 Alzheimer disease and mild cognitive impairment: a marker for disease severity. *Radiology*.  
463 2013;267(1):221-30.

464 32. Boban M, Crnac P, Junakovic A, Garami Z, Malojcic B. Blood flow velocity changes in anterior  
465 cerebral arteries during cognitive tasks performance. *Brain Cogn*. 2014;84(1):26-33.

466 33. Schuff N, Matsumoto S, Kmiecik J, Studholme C, Du A, Ezekiel F, et al. Cerebral blood flow in  
467 ischemic vascular dementia and Alzheimer's disease, measured by arterial spin-labeling magnetic  
468 resonance imaging. *Alzheimers Dement*. 2009;5(6):454-62.

469 34. Nation DA, Wierenga CE, Clark LR, Dev SI, Stricker NH, Jak AJ, et al. Cortical and subcortical  
470 cerebrovascular resistance index in mild cognitive impairment and Alzheimer's disease. *J Alzheimers*  
471 *Dis*. 2013;36(4):689-98.

472 35. Nortley R, Korte N, Izquierdo P, Hirunpattarasilp C, Mishra A, Jaunmuktane Z, et al. Amyloid  
473 beta oligomers constrict human capillaries in Alzheimer's disease via signaling to pericytes. *Science*.  
474 2019;365(6450).

475

## Figures

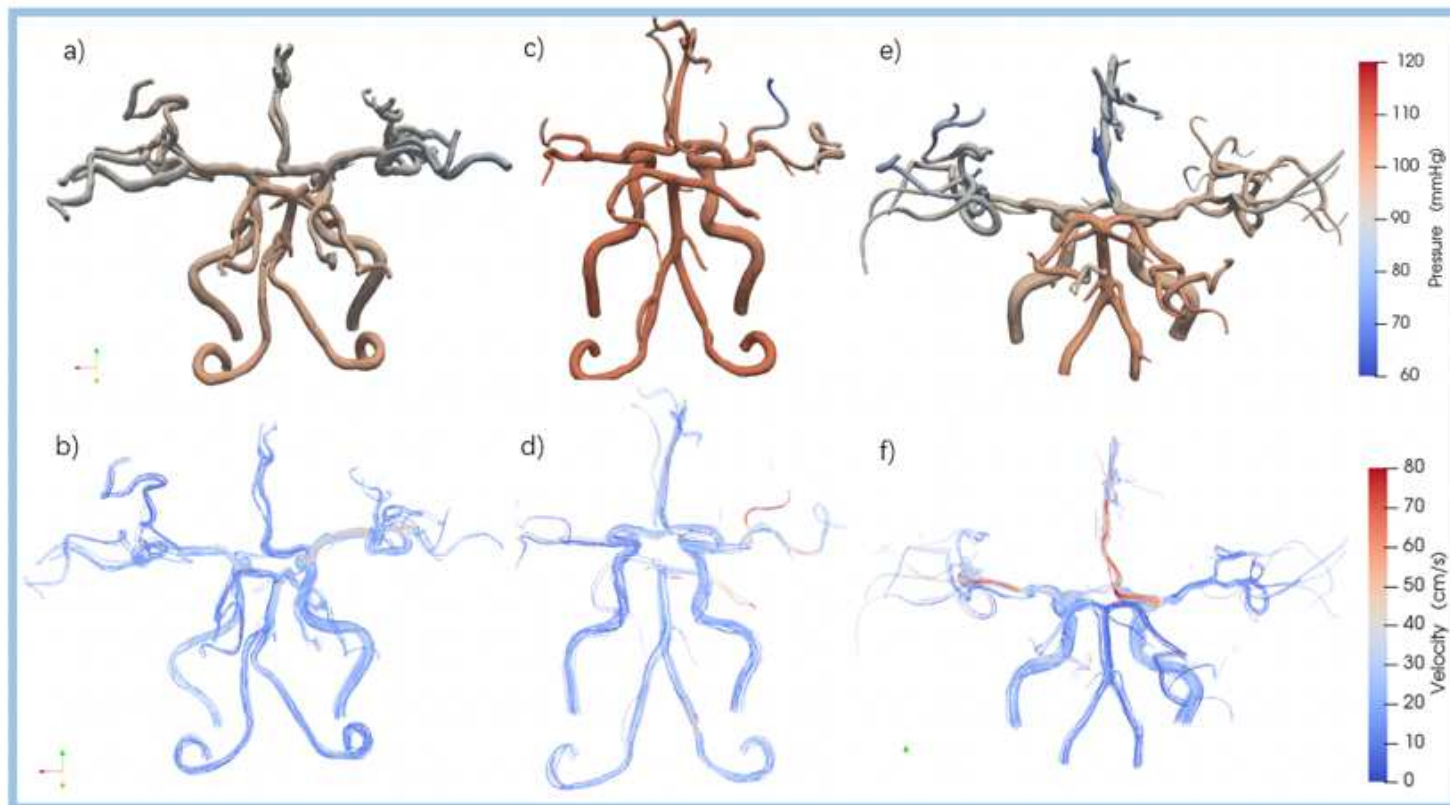


**Figure 1**

Three typical examples of pressure distribution and stream lines of blood flow velocity are displayed in the first and the second row, respectively. The first column( fig a and b )is for an AD patients, the second column (fig c and d )is for a VaD patients, and the third column (fig e and f) is for a healthy subject. It is evident that the AD patient and the healthy subject are with intact arterial trees, whereas VaD the patient is with scarce arterial branches. However, according to computation, the total blood flow in the models was 692 ml/min (AD patient), 647 ml/min (VaD patient), and 998 ml/min (healthy subject) respectively.

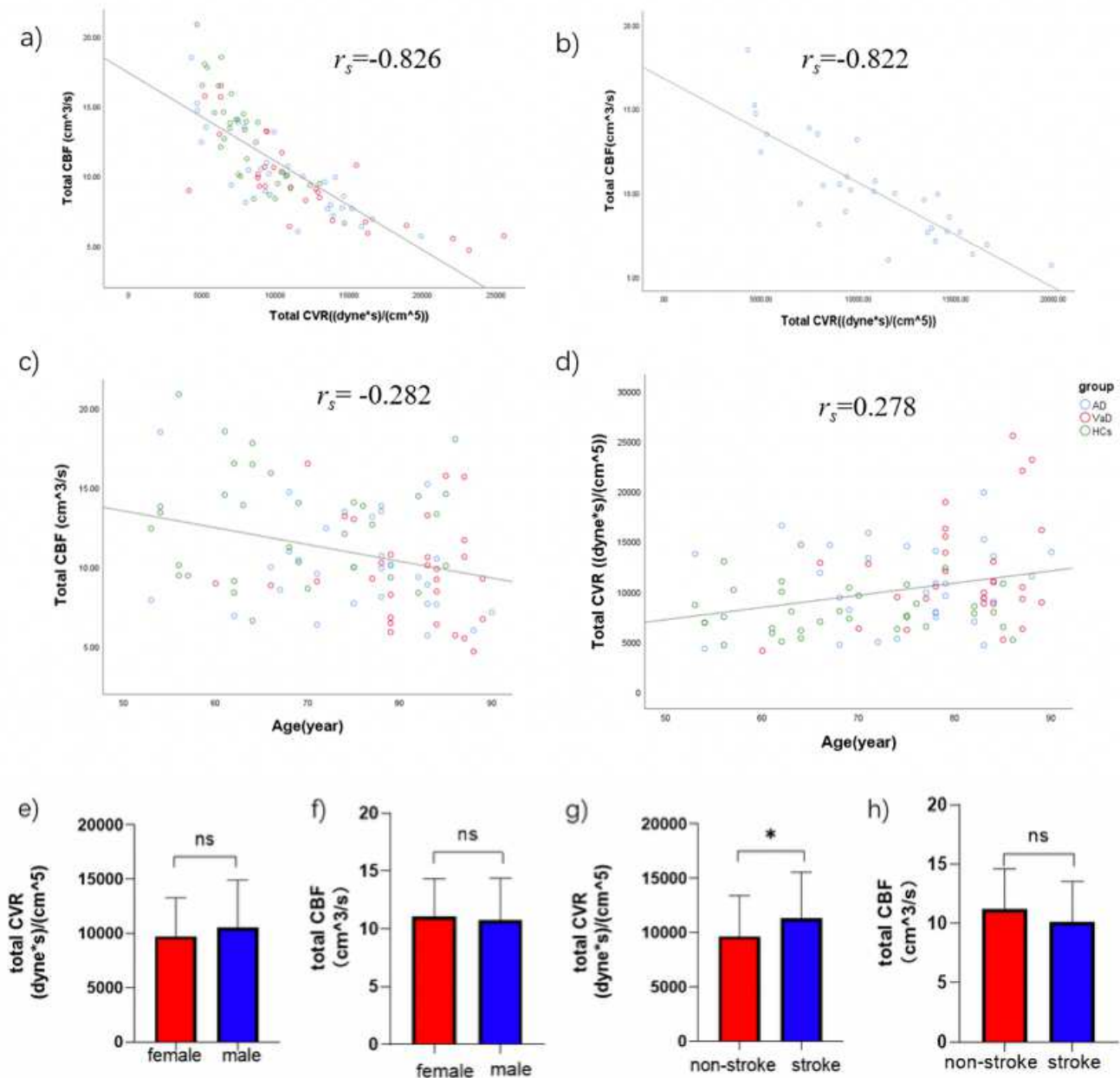


**Figure 2**

Interactive associations of the hemodynamic parameters and risk factors, correlation between total CBF and CVR in all subjects (a) and AD group(b), (c) and (d) showed significant correlations between CBF or CVR and age, fig(e, f) showed there were no significant difference of total CVR or CBF between male and female patients, fig(g) indicated there was significant difference of total CVR in patients with stroke or not, but not total CBF fig(h).ns: no significance, \*P<0.05.

## Supplementary Files

This is a list of supplementary files associated with this preprint. Click to download.

- [supplementarymaterial.docx](#)